

## Turing pattern formation induced by spatially correlated noise

Adolfo Sanz-Anchelergues,<sup>1</sup> Anatol M. Zhabotinsky,<sup>2</sup> Irving R. Epstein,<sup>2</sup> and Alberto P. Muñuzuri<sup>1,\*</sup>

<sup>1</sup>Group of Nonlinear Physics, Faculty of Physics, University of Santiago de Compostela, 15706 Santiago de Compostela, Spain

<sup>2</sup>Department of Chemistry and Volen Center for Complex Systems, Brandeis University, Waltham, Massachusetts 02454-9110

(Received 3 December 1999; revised manuscript received 21 August 2000; published 25 April 2001)

The effect of spatially correlated noise on Turing structures is analyzed both experimentally and numerically. Using the photosensitive character of the chlorine dioxide-iodine-malonic acid reaction-diffusion system, spatial randomness is introduced in the system. In the presence of noise, Turing patterns appear and are stable at levels of average illumination that would be more than sufficient to suppress pattern formation in the case of homogeneous illumination.

DOI: 10.1103/PhysRevE.63.056124

PACS number(s): 82.20.Mj, 47.20.Bp, 47.70.Fw

The symmetry-breaking spatial structures associated with the name of Alan Turing [1] arise when differences in diffusion rates cause an initially stable homogeneous system to become unstable to nonhomogeneous perturbations. This idea was developed by Turing in an effort to provide a chemical basis for biological structures and patterns such as those on animal coats. His mechanism has been utilized to describe pattern formation in semiconductor physics [2,3], star formation in galaxies [4], biological morphogenesis [5–7], etc. Despite the considerable interest in them, Turing structures were not observed experimentally until 1990 by DeKepper's group [8]. Since then, the dynamics of Turing structures in autonomous systems have been investigated in detail [9–11].

Experiments on Turing structures are most often done with the chlorite-iodide-malonic acid reaction [12] or its variant, the chlorine dioxide-iodine-malonic acid (CDIMA) reaction [13]. Only recently, the photosensitivity of the CDIMA reaction has been established [14] and used to study the behavior of Turing patterns in the presence of periodic homogeneous external forcing [15,16].

The effect of stochasticity on pattern formation has been widely studied in recent years [17–20]. Noise has been found to be a significant factor in determining the spatiotemporal behavior of these patterns in oscillatory reactions, such as the Belousov-Zhabotinsky reaction-diffusion systems [22,21]. In spite of these efforts, the corresponding behavior of Turing structures remains almost unstudied. In this paper, the photosensitivity of the CDIMA reaction allows us to impose stochastic patterns that locally modulate the control parameters of the system.

Experiments were carried out in a thermostatted one-sided continuously fed unstirred reactor [15,11,23] at  $4 \pm 1^\circ\text{C}$ . Structures appeared in a polyacrylamide gel layer (thickness 0.3 mm) with immobilized starch (0.5% weight/volume) separated from the feeding chamber by an Anapore membrane (Whatman, pore size  $0.2 \mu\text{m}$ ) and a nitrocellulose membrane (Schleicher and Schnell, pore size  $0.45 \mu\text{m}$ ). The reagents were fed into the feeding chamber by a peristaltic pump. The input concentrations were; 0.35 mM  $\text{I}_2$  (dissolved in 30% acetic acid), 0.185 mM  $\text{ClO}_2$ , 10 mM

$\text{H}_2\text{SO}_4$ , and 1.5 mM malonic acid. The feeding chamber residence time was set equal to 90 s for all experiments. Two magnetic stirrers placed in the feeding chamber ensured the homogeneity of the solution in contact with the gel.

The gel layer was illuminated with unfiltered light from a tungsten-halogen lamp. The nonuniformity of the light field was less than 10%. The light intensity reaching the system  $\phi$ , was varied from 0 to 11 mW/cm<sup>2</sup>. Above 40%  $\pm 5\%$  (4.5 mW/cm<sup>2</sup>) of the maximum intensity, the Turing structures were inhibited. In order to stochastically modulate the conditions in the medium, the light  $\phi$ , reaching the gel was projected through a transparency imprinted with a pattern of randomly distributed black and transparent squares (black and white from now on) of length  $l$ . The transmittance for each square was set equal to either  $T_o - \delta T$  for the black squares (with probability of occurrence  $p$ ) or  $T_o + \delta T$  for the white squares (with probability of occurrence  $q = 1 - p$ ), where  $T_o$  is a reference value of transmittance (equal to the mean value of transmittance for the case  $p = q$ ). Thus, the transmittance function  $T(i, j)$  can be written as

$$T(i, j) = T_o + \delta T \eta(i, j) \quad i, j = 1, \dots, N, \quad (1)$$

where  $i$  and  $j$  are the coordinates for each square and  $N$  is the maximum number of squares in the transparency for each direction.  $\eta(i, j) = \pm 1$  is a two-valued random number with average equal to  $q - p$ . The mean transmittance is, then, given by

$$\langle T(i, j) \rangle = T_o + \delta T(1 - 2p). \quad (2)$$

Each transparency is characterized by three parameters; the spatial correlation length  $l$ , or the size of the squares projected on the gel, the noise intensity,  $\delta T$  (that gives information about the deviation of the light intensity from the mean value), and the probability of black squares  $p$ , or squares with transmittance  $T_o - \delta T$ .

Standard protocol for the first set of experiments always kept the average value of the light intensity in the medium constant and equal to 50% of the maximum (11 mW/cm<sup>2</sup>) and the parameter varied was  $l$ ; the average illumination level was, then, sufficient to suppress Turing pattern formation. Illumination was applied to the gel layer for 4 h, and the pattern obtained was recorded after that time with a CCD videocamera. In all experiments, part of the medium was

\*Author to whom correspondence should be addressed. Email address: uscfmapm@cesga.es; http://chaos.usc.es

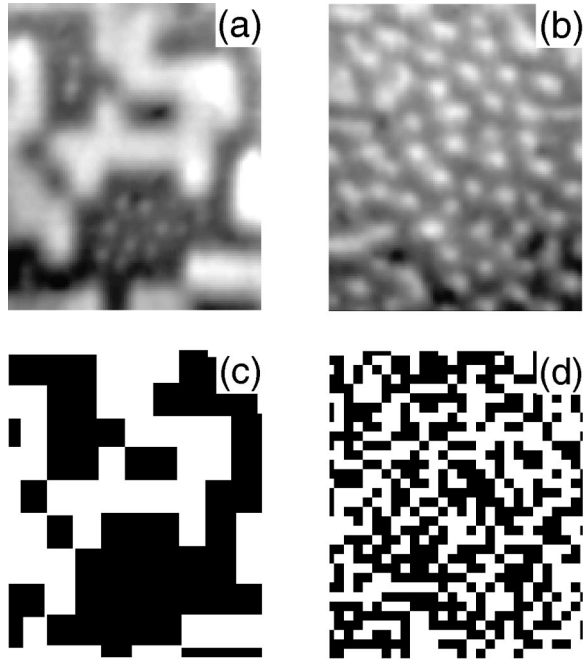


FIG. 1. Noise-induced Turing patterns in the photosensitive CDIMA reaction. (a)  $l=0.35$  mm, Turing structures just appear in the areas in darkness forming clusters of structures, (b)  $l=0.09$  mm, Turing structures covering the whole medium, (c) pattern of illumination projected onto the reactor corresponding with the experiment in Fig. 1(a), and (d) pattern of illumination projected onto the reactor corresponding with the experiment in Fig. 1(b). ( $\phi_o=50\%$   $\phi_{max}=5.5$  mW/cm<sup>2</sup>,  $\delta\phi=5.5$  mW/cm<sup>2</sup> =  $50\%$   $\phi_{max}$ , wavelength,  $\lambda=0.32\pm 0.05$  mm).

kept in darkness (with the rest illuminated through the transparency as explained above) in order to measure the wavelength of the Turing structures free from any external influence; in this way, we could ensure that the system parameters did not change from experiment to experiment. For our experimental conditions and with no external influence, hexagons appeared spontaneously with a wavelength  $\lambda=0.32\pm 0.05$  mm.

Different experimental results were observed when changing the correlation length  $l$  (Fig. 1). For large values of  $l$  ( $l>0.21\pm 0.04$  mm) Turing structures appeared only in the nonilluminated areas [Fig. 1(a)] forming a sort of clusters of Turing structures. In Fig. 1(a), the white areas correspond to the illuminated areas while the darker areas are nonilluminated. The spots in these latter areas are Turing structures. The pattern of illumination projected onto the reactor is shown in Fig. 1(c), note that only where accumulation of black squares occurs, Turing structures arise [Fig. 1(a)]. For intermediate values of  $l$ , Turing patterns appeared homogeneously distributed throughout the gel [Fig. 1(b)]; here, because the Turing patterns are distributed over the system, the transmittance pattern [shown in Fig. 1(d)] cannot be seen in the figure. For small  $l$  ( $l<0.04\pm 0.02$  mm  $\ll \lambda=0.32\pm 0.05$  mm) no structure appeared. Experiments were run at least three times for each value of  $l$ . Since the average value of the applied illumination lies well above the transition to the homogeneous state, the existence of Turing patterns must

result from the randomness introduced in the medium through illumination.

To compare the experimental results with those from numerical simulations, we employed the Lengyel-Epstein two-variable model [23,24] modified to include the effect of illumination [14]

$$\begin{aligned} \dot{u} &= a - cu - 4\frac{uv}{1+u^2} - \phi + \nabla^2 u, \\ \dot{v} &= \sigma \left( cu - \frac{uv}{1+u^2} + \phi + d\nabla^2 v \right). \end{aligned} \quad (3)$$

Here,  $u$  and  $v$  are the dimensionless concentrations of I<sup>-</sup> and ClO<sub>2</sub><sup>-</sup>, respectively;  $a$ ,  $c$ , and  $\sigma$  are dimensionless parameters proportional to other initial concentrations and rate constants, and  $d$  is the ratio of the diffusion constants in the absence of starch [24,14].  $\phi$  is the dimensionless rate of the photochemical reaction, which is proportional to the light intensity.  $\phi$  depends on the position (as in the experimental case) and it is proportional to the transmittance function [Eq. (2)]. Thus, for the white squares  $\phi = \phi_o + \delta\phi$  (with probability of occurrence  $q=1-p$ ) and for the black squares  $\phi = \phi_o - \delta\phi$  (with probability of occurrence  $p$ ).  $\delta\phi$  contains the information of the noise intensity and  $\phi_o$  is a reference value of light intensity (as in the experimental case). The critical Turing wave number in terms of the model parameters is

$$k_c^2 = \frac{1}{2} \left( \frac{4v_o(u_o^2 - 1)}{1 + u_o^2} - c - \frac{u_o}{d(1 + u_o^2)} \right) \quad (4)$$

with  $u_o = (a - 5\phi)/(5c)$  and  $v_o = a(1 + u_o^2)/(5u_o)$  denoting the steady-state values of  $u$  and  $v$ .

In our simulations, we fixed  $a=16$ ,  $c=0.6$ ,  $\sigma=301$ , and  $d=1.07$  (these values correspond to the initial reagent concentrations used in the experiments). With these values we recovered the three different types of experimental behaviors observed (Fig. 2). The transition between Turing structures and the homogeneous state under homogeneous illumination occurs at  $\phi=2.3$ . In the simulations of Fig. 2, we set  $\phi_o=2.4$  and  $\delta\phi=0.15$ . Thus, the average illumination was well above the transition value ( $\phi=2.3$ ) and the effect shown in Fig. 2(b) arises solely from the stochasticity in the medium.

So far, we have considered only  $l$  as an adjustable parameter. We also varied the other parameters, i.e.,  $\delta\phi$  and  $\phi_o$ . In Fig. 3 we show the boundaries in the parameter space of the regions where the three different behaviors occur. To define the boundary between Turing and no-pattern regions, we considered Turing structures to exist when the amplitude of the peaks was larger than  $1.2 \times [u_o(\phi = \phi_o - \delta\phi) - u_o(\phi = \phi_o + \delta\phi)]$  [with  $u_o$  defined as in Eq. (5)]. In this way, we distinguish real Turing patterns from simple noise due to a change in the level of illumination. The boundary between the Turing structure region and the clusters of Turing structures was calculated by comparing the areas containing Turing structures and the areas illuminated. If all the structures

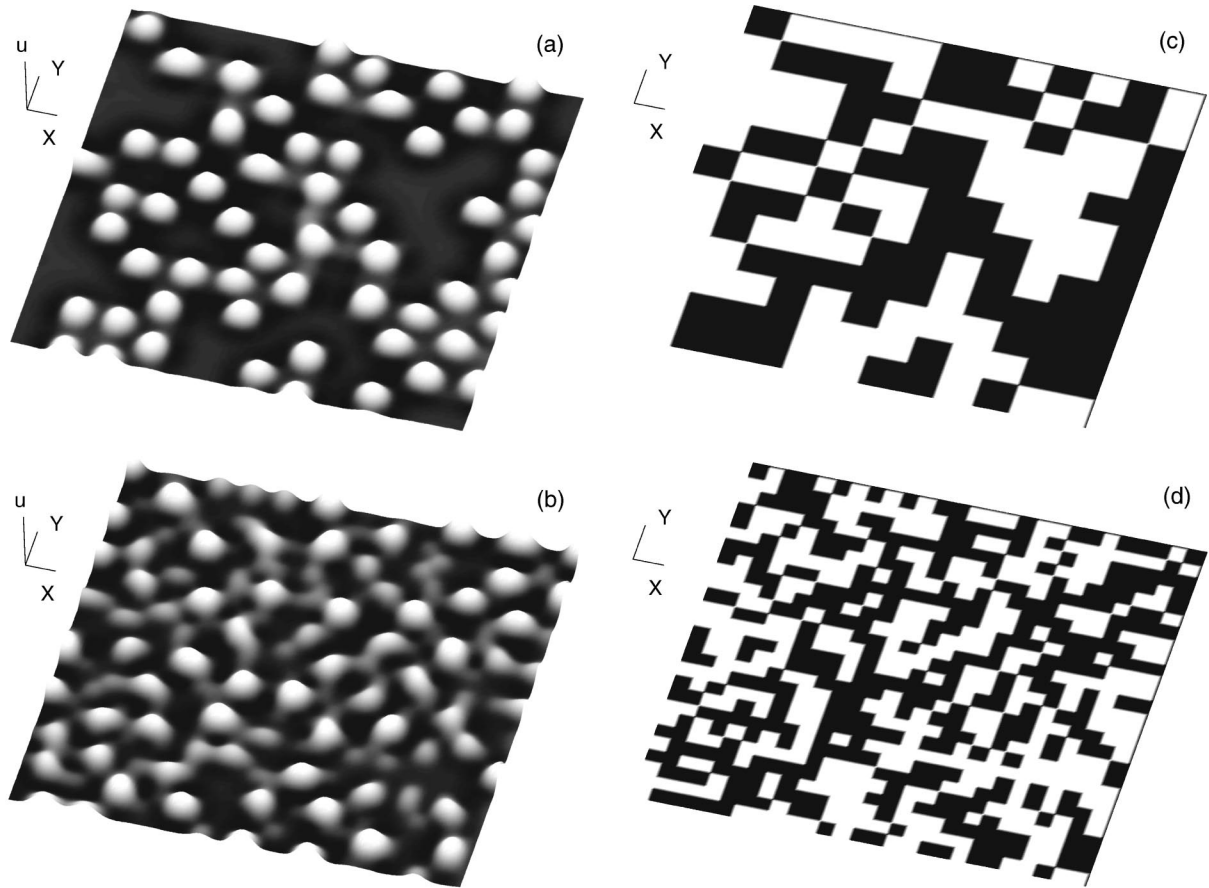


FIG. 2. Noise induced Turing structures in the Lengyel-Epstein two-variable model modified to include the effect of illumination. (a)  $l=5.0$  spatial units (s.u.), Turing structures just appear in the areas in darkness forming clusters of structures, (b)  $l=2.2$  s.u., Turing structures covering the whole medium, (c) pattern of illumination projected onto the system corresponding with the simulation shown in Fig. 2(a), and (d) pattern of illumination projected onto the system corresponding with the simulation shown in Fig. 2(b). ( $\phi_o=2.4$ ,  $\delta\phi=0.15$ , wavelength,  $\lambda=6.8$  s.u.).

lay in the nonilluminated region then we concluded that clusters of Turing structures had appeared.

In the previous results, we only considered the case with  $p=q$ , i.e., the probability of black and white squares is equal. The influence of a variation in  $p$  is shown in Fig. 4 where experimental and numerical results are presented. We define the normalized density of spots (NDS) as the measured density of Turing peaks in a region, normalized by the density of spots in the reference area (that was kept in darkness, i.e.,  $\phi = \phi_o - \delta\phi$ ). Figure 4 shows the values of NDS measured for different values of  $p$  in experiments [Fig. 4(a)] and numerics [Fig. 4(b)]. All other parameters were kept constant. For small values of  $p$  almost the whole medium is illuminated and very few structures develop while for large values of  $p$  almost everywhere is in darkness and structures cover the whole medium. Notice that, in both cases, there is a sudden increase in NDS for  $p=0.3$  (for  $p>0.3$ , spots cover homogeneously the whole medium).

In this paper we have presented results showing that stochasticity plays an important role in determining whether Turing structures may appear. Randomness in the system parameters stabilizes Turing structures far from their normal regions of stability. In the present paper the effect of dichot-

omous noise on the medium was analyzed. We found that the square size,  $l$  is the crucial parameter. For  $l$  much smaller than the wavelength of the Turing structures ( $\lambda \cong 2\pi/k_c$ ), the system senses an effective homogeneous light intensity equal to the mean value (50%) and no structure can appear. As  $l$  is increased, Turing structures appear homogeneously distributed over the system. Although  $l$  is smaller than  $\lambda$ , the probability of forming clusters of black squares increases and their effective size becomes comparable to  $\lambda$ . For this range of values of  $l$ , the noise in the medium stabilizes Turing structures far from the range of stability for homogeneous illumination [see Fig. 1(b)].

For large values of  $l$ , the black squares have a high probability of forming clusters. Their effective size thus becomes much larger than  $\lambda$ , and several Turing spots may fit into the black clusters. Here, regions illuminated and in darkness are clearly separated and Turing structures appear only in the dark clusters [see Fig. 1(a)].

It is important to note that the appearance of Turing structures here reported is induced by the spatially correlated noise under conditions where the average light intensity is strong enough to suppress pattern formation. This mechanism is not directly related to the formation of localized

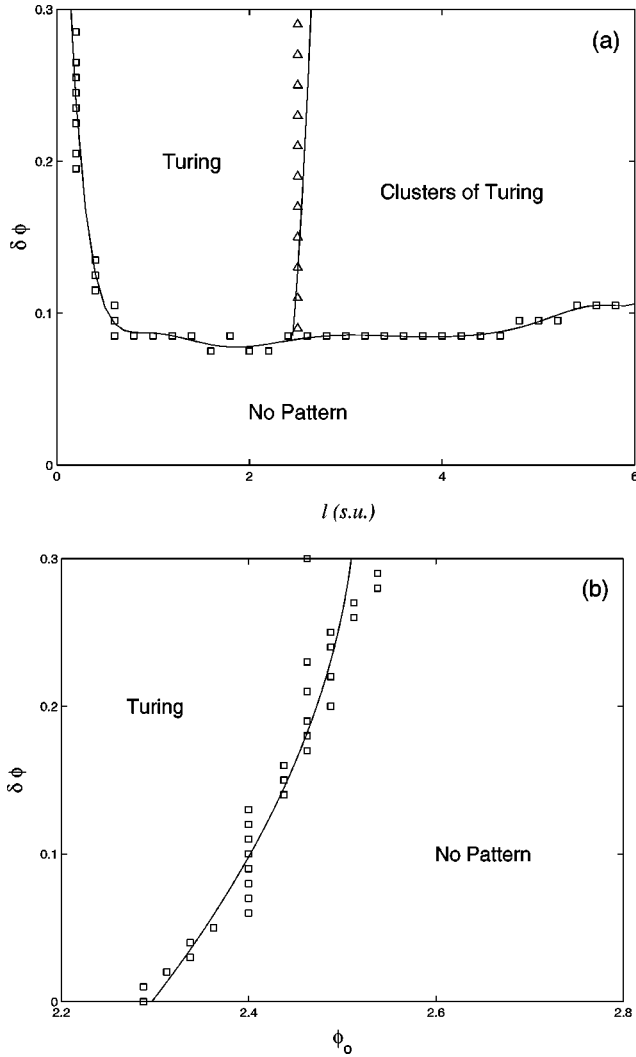


FIG. 3. Numerical phase diagrams. (a)  $\delta\phi$  vs  $l$  diagram ( $\phi_o = 2.4$ ). (b)  $\delta\phi$  vs  $\phi_o$  diagram ( $l = 1.0$  s.u.). The regions correspond with the three behaviors observed in Figs. 1 and 2, namely, no-pattern or noise, Turing, and clusters of Turing structures. (Squares,  $\square$ , mark the transition from Turing structures to no pattern while triangles,  $\triangle$ , mark the transition to clusters of structures. Solid lines are to guide the eyes.) (Illumination threshold, above which no pattern can appear when constant illumination is applied, is 2.3).

structures in a subcritical bifurcation [25,26]. Actually, we performed experiments increasing homogeneously the light intensity  $\phi$ , reaching the medium and structures disappeared for light values above 40% of the maximum ( $\phi_{max}$ ) (while for the experiments in Fig. 1 we always kept  $\langle\phi\rangle = 50\% \phi_{max}$ ).

Other values of  $\delta\phi$  and  $\phi_o$  were also used in simulations

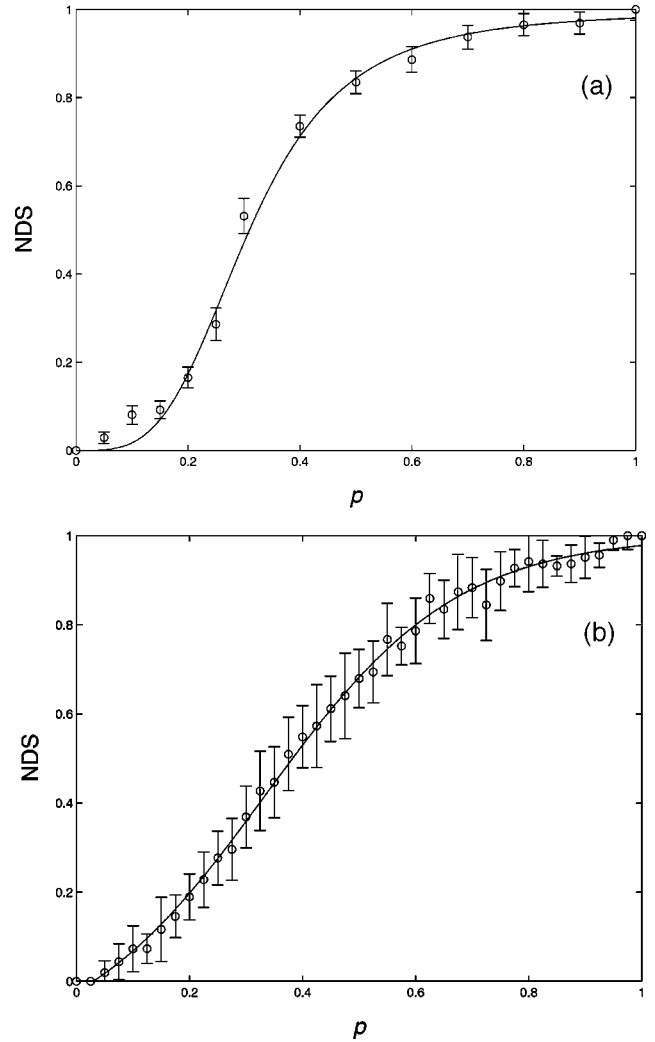


FIG. 4. Normalized density of spots (NDS), versus  $p$ , (a) experimental ( $l = 0.09$  mm,  $\phi_o = 50\% \phi_{max} = 5.5$  mW/cm<sup>2</sup>, and  $\delta\phi = 5.5$  mW/cm<sup>2</sup> = 50%  $\phi_{max}$ ; each point in the figure was averaged over at least three experiments) and (b) numerical ( $l = 1.0$  s.u.,  $\phi_o = 2.4$  and  $\delta\phi = 0.16$ ; each point was averaged over 12 runs to reduce finite-size statistical dispersion). Solid lines are guides to the eye.

to show that this phenomenon is general and independent of the model parameters.

Here, we have considered only simple, dichotomous spatial noise and have shown that it is capable of dramatically enlarging the region of the stability of Turing structures. More interesting phenomena may be expected when spatiotemporal correlated noise is introduced.

This work was partially supported by MCYT under Research Grant No. BFM-2000-0348.

- [1] A. M. Turing, *Philos. Trans. R. Soc. London, Ser. B* **B237**, 37 (1952).  
 [2] B. Röhrich, J. Parisi, J. Peinke, and O. E. Rössler, *Z. Phys. B: Condens. Matter* **65**, 259 (1986).

- [3] Y. I. Balkarei, A. V. Grigor'yants, Y. A. Rzhanov, and M. I. Elinson, *Opt. Commun.* **66**, 161 (1988).  
 [4] T. Nozakura and S. Ikeuchi, *Astrophys. J.* **279**, 40 (1984).  
 [5] H. Meinhardt, *Models of Biological Pattern Formation* (Aca-

- demic, London, 1982).
- [6] J. D. Murray, *Mathematical Biology* (Springer-Verlag, Berlin, 1989).
- [7] L. Edelstein-Keshet, *Mathematical Models in Biology* (Random House, New York, 1988).
- [8] V. Castets, E. Dulos, J. Boissonade, and P. DeKepper, *Phys. Rev. Lett.* **64**, 2953 (1990).
- [9] *Chemical Waves and Patterns*, edited by R. Kapral and K. Showalter (Kluwer Academic, Dordrecht, 1995).
- [10] Q. Ouyang and H. L. Swinney, *Nature (London)* **352**, 610 (1991).
- [11] B. Rudovics, E. Barillot, P. Davies, E. Dulos, J. Boissonade, and P. DeKepper, *J. Phys. Chem.* **103**, 1790 (1999).
- [12] P. DeKepper, I. R. Epstein, K. Kustin, and M. Orbán, *J. Phys. Chem.* **86**, 170 (1982).
- [13] I. Lengyel, G. Rabai, and I. R. Epstein, *J. Am. Chem. Soc.* **112**, 4606 (1990); *ibid.* **112**, 9104 (1990).
- [14] A. P. Muñuzuri, M. Dolnik, A. M. Zhabotinsky, and I. R. Epstein, *J. Am. Chem. Soc.* **121**, 8065 (1999).
- [15] A. Horváth, M. Dolnik, A. P. Muñuzuri, A. M. Zhabotinsky, and I. R. Epstein, *Phys. Rev. Lett.* **83**, 2950 (1999).
- [16] M. Dolnik, A. M. Zhabotinsky, and I. R. Epstein, *Phys. Rev. E* **63**, 026101 (2001).
- [17] A. S. Mikhailov, L. Schimansky-Geier, and W. Ebeling, *Phys. Rev. Lett.* **96A**, 453 (1983).
- [18] J. Maselko and K. Showalter, *Physica D* **49**, 21 (1991).
- [19] P. Jung and G. Mayer-Kress, *Phys. Rev. Lett.* **74**, 2130 (1995).
- [20] J. García-Ojalvo and J. M. Sancho, *Noise in Spatially Extended Systems* (Springer-Verlag, New York, 1999).
- [21] I. Sendiña-Nadal, A. P. Muñuzuri, D. Vives, V. Pérez-Muñuzuri, J. Casademunt, L. Ramírez-Piscina, J. M. Sancho, and F. Sagués, *Phys. Rev. Lett.* **80**, 5437 (1998).
- [22] I. Sendiña-Nadal, S. Alonso, V. Pérez-Muñuzuri, M. Gómez-Gesteira, V. Pérez-Villar, L. Ramírez-Piscina, J. Casademunt, J. M. Sancho, and F. Sagués, *Phys. Rev. Lett.* **84**, 2734 (2000).
- [23] I. Lengyel, S. Kádár, and I. R. Epstein, *Phys. Rev. Lett.* **69**, 2729 (1992).
- [24] I. Lengyel and I. R. Epstein, *Science* **251**, 650 (1991); **259**, 493 (1993).
- [25] O. Jensen, V. O. Pannbacker, E. Mosekilde, G. Dewel, and P. Borckmans, *Phys. Rev. E* **50**, 736 (1994).
- [26] O. Jensen, E. Mosekilde, P. Borckmans, and G. Dewel, *Phys. Scr.* **53**, 243 (1996).